

Supporting Information

Synthesis, Photophysical, and Magnetic Studies of Ternary Lanthanide(III) Complexes of Naphthyl Chromophore Functionalized Imidazo[4,5-*f*][1,10]-phenanthroline and Dibenzoylmethane

A. Josephine Kanimozhi and V. Alexander*

Department of Chemistry, Loyola College, Chennai-600034, India.

Table of Contents

	<i>Page</i>
Figure S1. ESI-TOF mass spectrum of L1	3
Figure S2. ESI-TOF mass spectrum of L2	4
Figure S3. 500 MHz ^1H NMR spectrum of L1 in $\text{DMSO}-d_6$ at 25 °C	5
Figure S4. ^1H - ^1H COSY spectrum of L1	6
Figure S5. 500 MHz ^1H NMR spectrum of L2 in $\text{DMSO}-d_6$ at 25 °C	7
Figure S6. ^1H - ^1H COSY spectrum of L2	8
Figure S7. 125 MHz ^{13}C NMR spectrum of L1 in $\text{DMSO}-d_6$ at 25 °C	9
Figure S8. 125 MHz ^{13}C NMR spectrum of L2 in $\text{DMSO}-d_6$ at 25 °C	10
Figure S9. Unit cell packing diagram displaying hydrogen bonding of L1	11
Figure S10. Unit cell packing diagram displaying hydrogen bonding of L2	12
Figure S11. ESI-TOF mass spectrum of $[\text{Eu}(\text{DBM})_3(\text{H}_2\text{O})_2]$	13
Figure S12. ESI-TOF mass spectrum of $[\text{Tb}(\text{DBM})_3(\text{H}_2\text{O})_2]$	14
Figure S13. ESI-TOF mass spectrum of $[\text{Eu}(\text{DBM})_3(\text{L1})]$	15
Figure S14. MALDI-TOF mass spectrum of $[\text{Tb}(\text{DBM})_3(\text{L1})]$	16
Figure S15. MALDI-TOF mass spectrum of $[\text{Eu}(\text{DBM})_3(\text{L2})]$	17
Figure S16. ESI mass spectrum of $[\text{Tb}(\text{DBM})_3(\text{L2})]$	18

Figure S17.	500 MHz ^1H NMR spectrum of $[\text{Eu}(\text{DBM})_3(\text{L1})]$ in $\text{DMSO}-d_6$ at 25°C	19
Figure S18.	500 MHz ^1H NMR spectrum of $[\text{Eu}(\text{DBM})_3(\text{L2})]$ in $\text{DMSO}-d_6$ at 25°C	20
Figure S19.	500 MHz ^1H NMR spectrum of $[\text{Tb}(\text{DBM})_3(\text{L1})]$ in $\text{DMSO}-d_6$ at 25°C	21
Figure S20.	500 MHz ^1H NMR spectrum of $[\text{Tb}(\text{DBM})_3(\text{L2})]$ in $\text{DMSO}-d_6$ at 25°C	22
Figure S21.	TGA curve of the complexes in N_2 atmosphere	23
Figure S22.	Electronic absorption spectra of L1 and L2	24
Figure S23.	Photoluminescence spectra of L1 and L2	25
Figure S24.	Excitation spectrum of L1 and L2	26
Figure S25.	Excitation spectra of $[\text{Eu}(\text{DBM})_3(\text{L1})]$ and $[\text{Eu}(\text{DBM})_3(\text{L2})]$	27
Figure S26.	Excitation spectra of $[\text{Tb}(\text{DBM})_3(\text{L1})]$ and $[\text{Tb}(\text{DBM})_3(\text{L2})]$	28
Figure S27.	Luminescence decay curves of $[\text{Eu}(\text{DBM})_3(\text{L1})]$ and $[\text{Eu}(\text{DBM})_3(\text{L2})]$	29

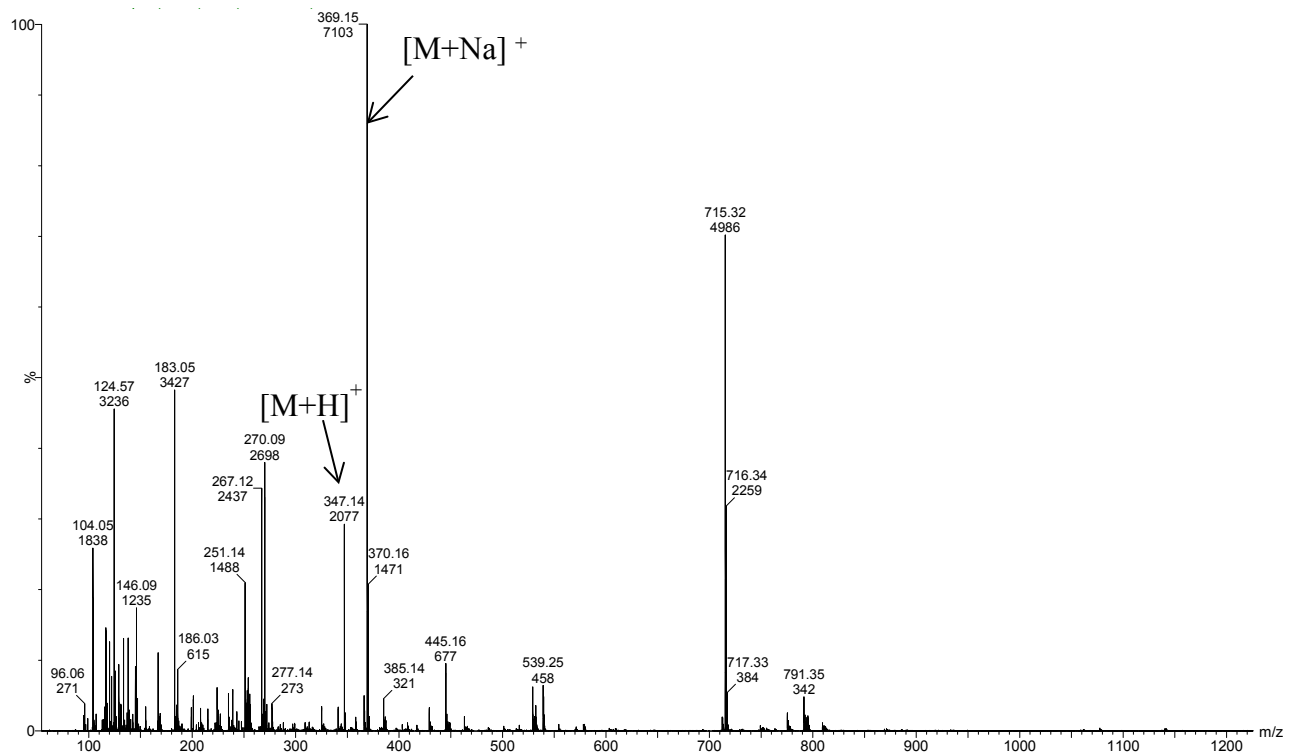


Figure S1. ESI-TOF mass spectrum of **L1**.

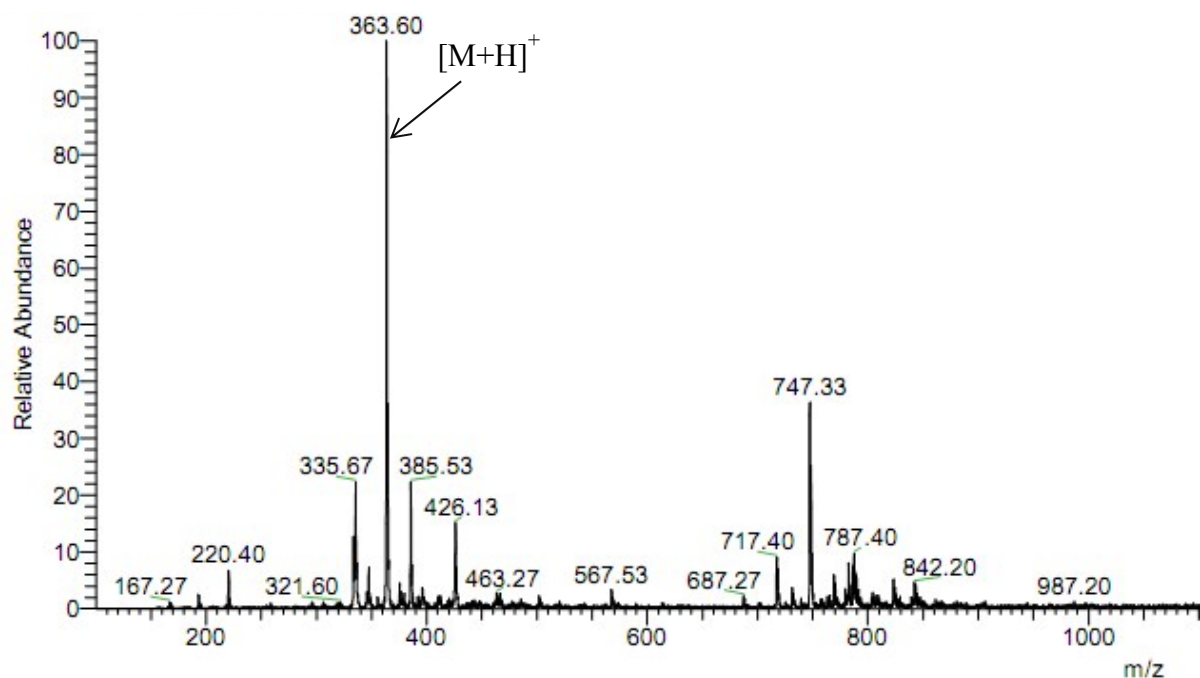


Figure S2. ESI-TOF mass spectrum of **L2**.

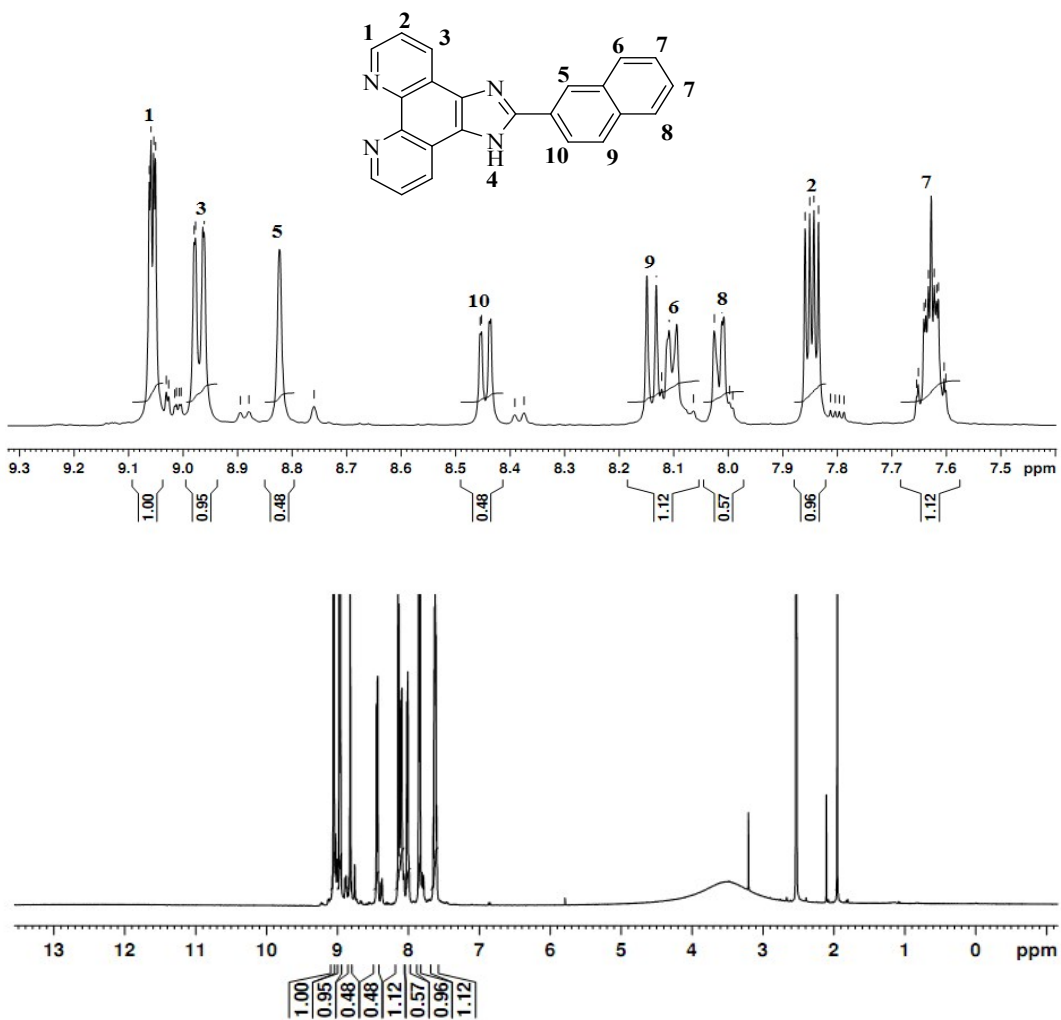


Figure S3. 500 MHz ^1H NMR spectrum of **L1** in $\text{DMSO}-d_6$ at 25°C .

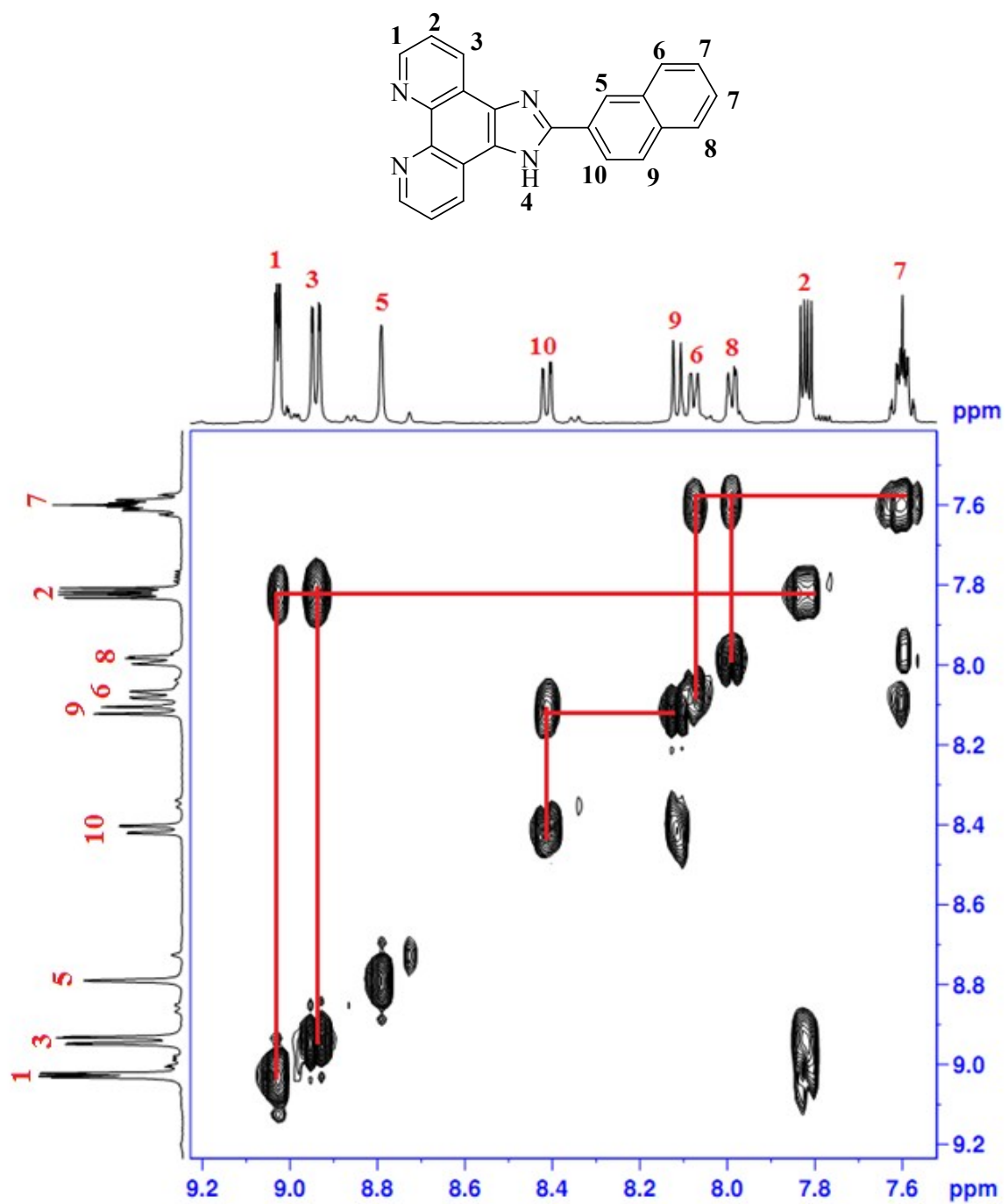


Figure S4. ^1H - ^1H COSY spectrum of L1.

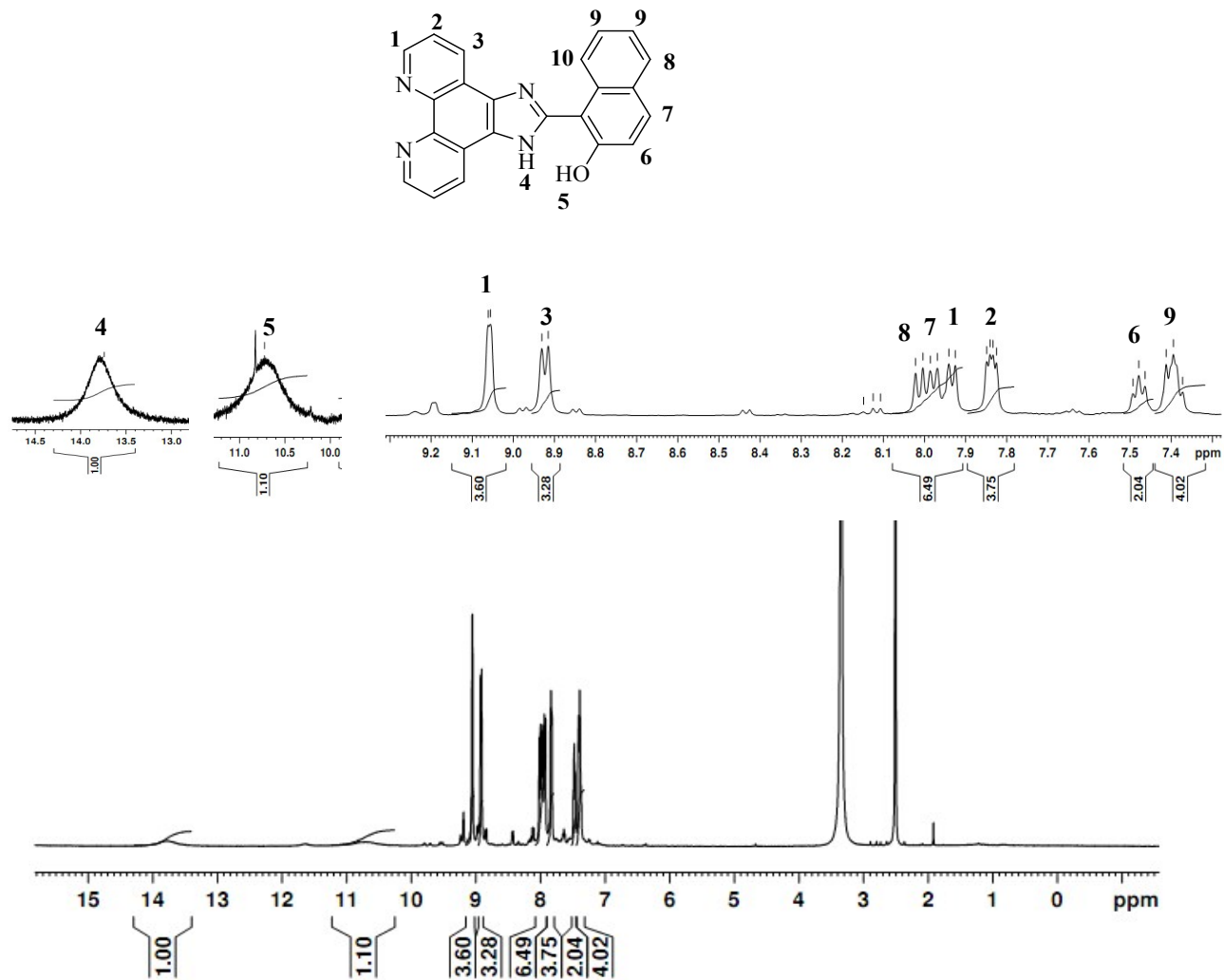


Figure S5. 500 MHz ^1H NMR spectrum of **L2** in $\text{DMSO}-d_6$ at 25 °C.

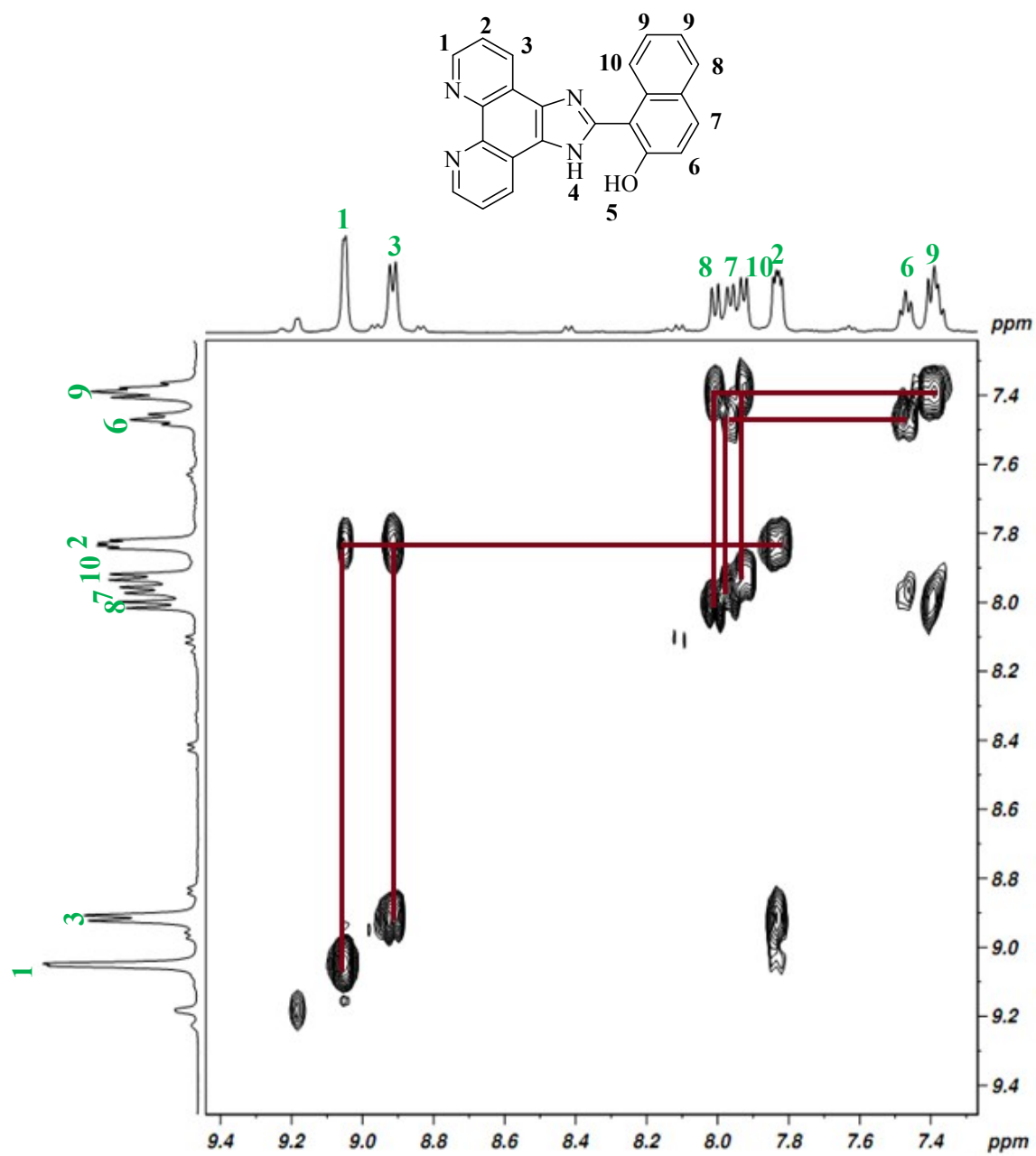


Figure S6. ^1H - ^1H COSY spectrum of L2.

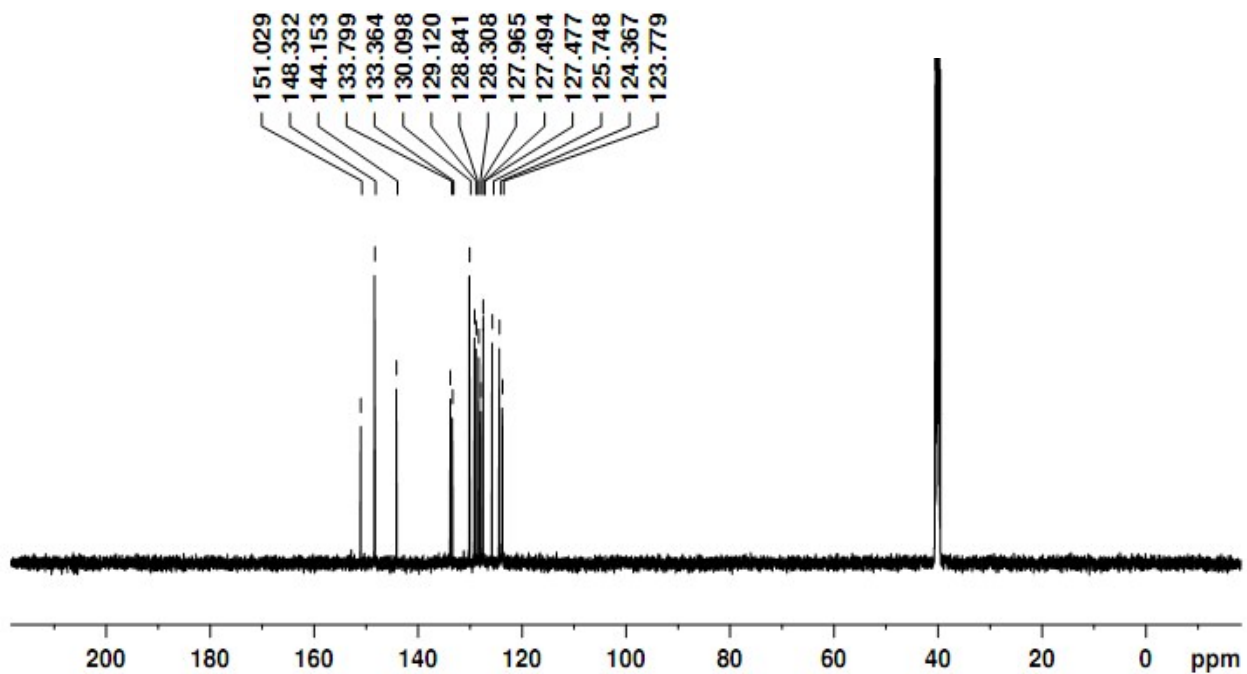


Figure S7. 125 MHz ^{13}C NMR spectrum of **L1** in $\text{DMSO}-d_6$ at 25 °C.

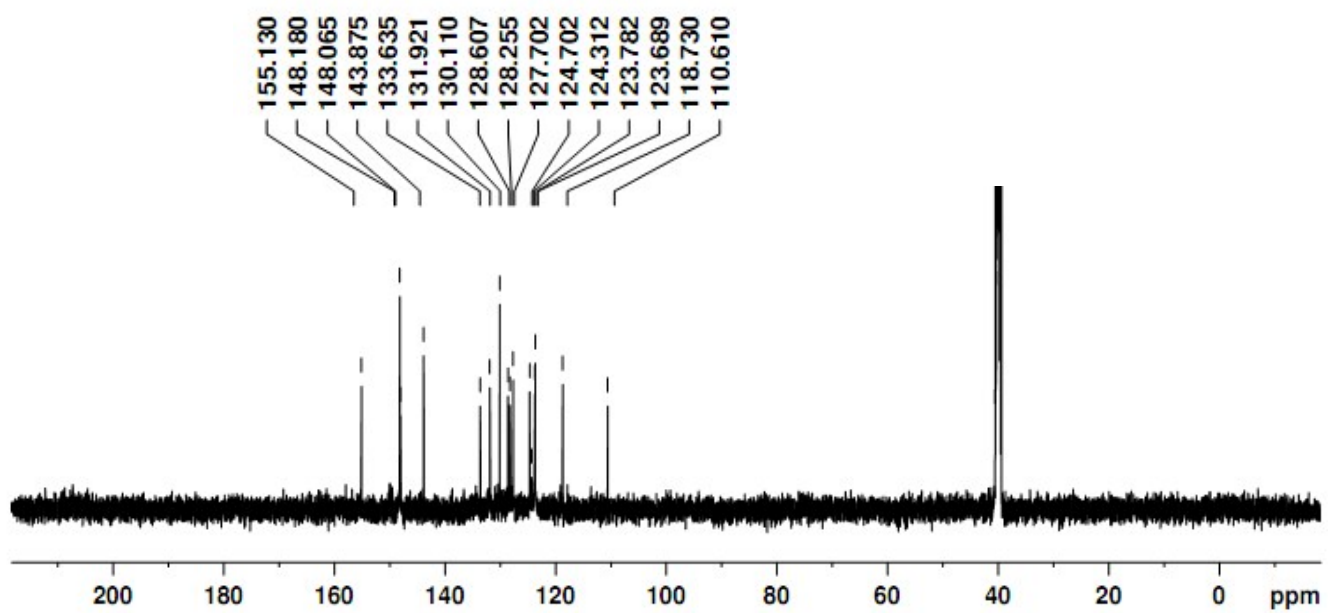


Figure S8. 125 MHz ^{13}C NMR spectrum of **L2** in $\text{DMSO}-d_6$ at 25 °C.

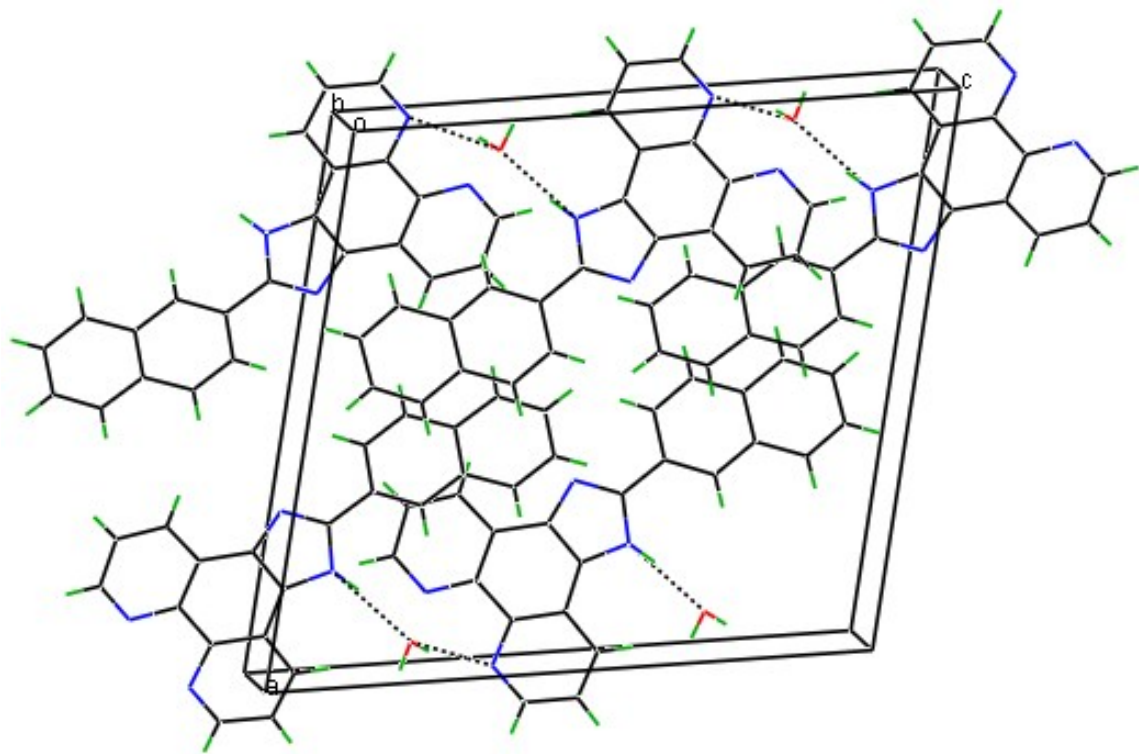


Figure S9. Unit cell packing diagram displaying hydrogen bonding of **L1**.

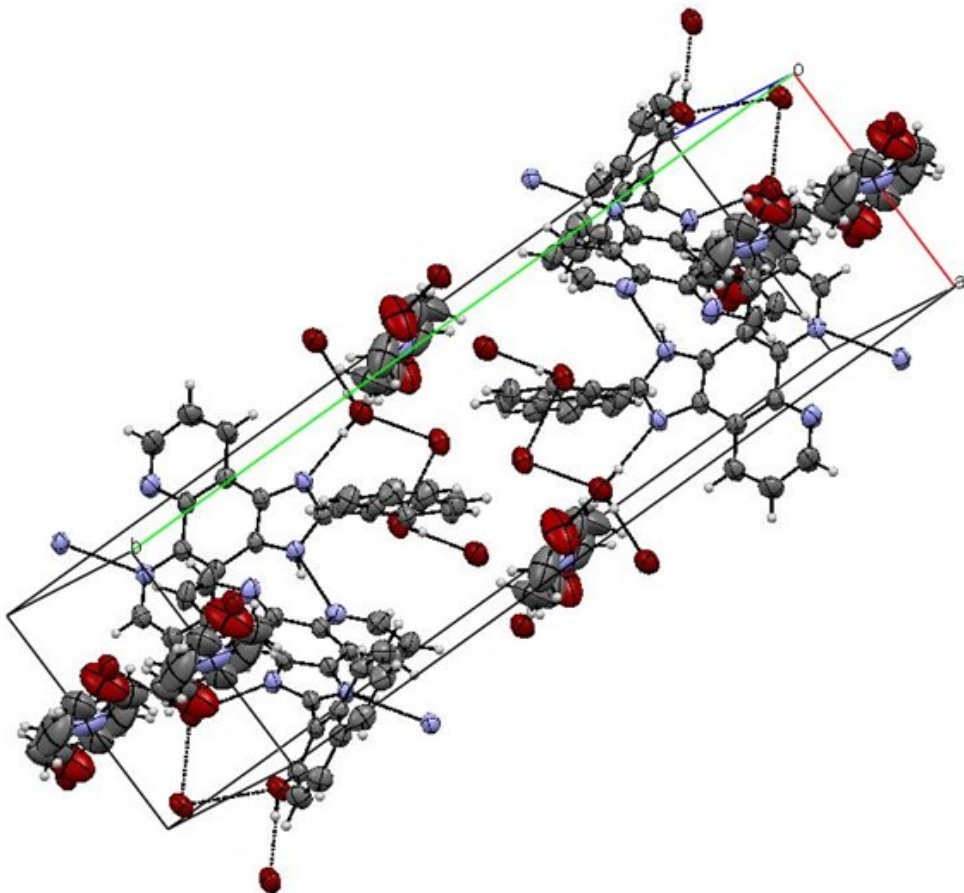


Figure S10. Unit cell packing diagram displaying hydrogen bonding of **L2**.

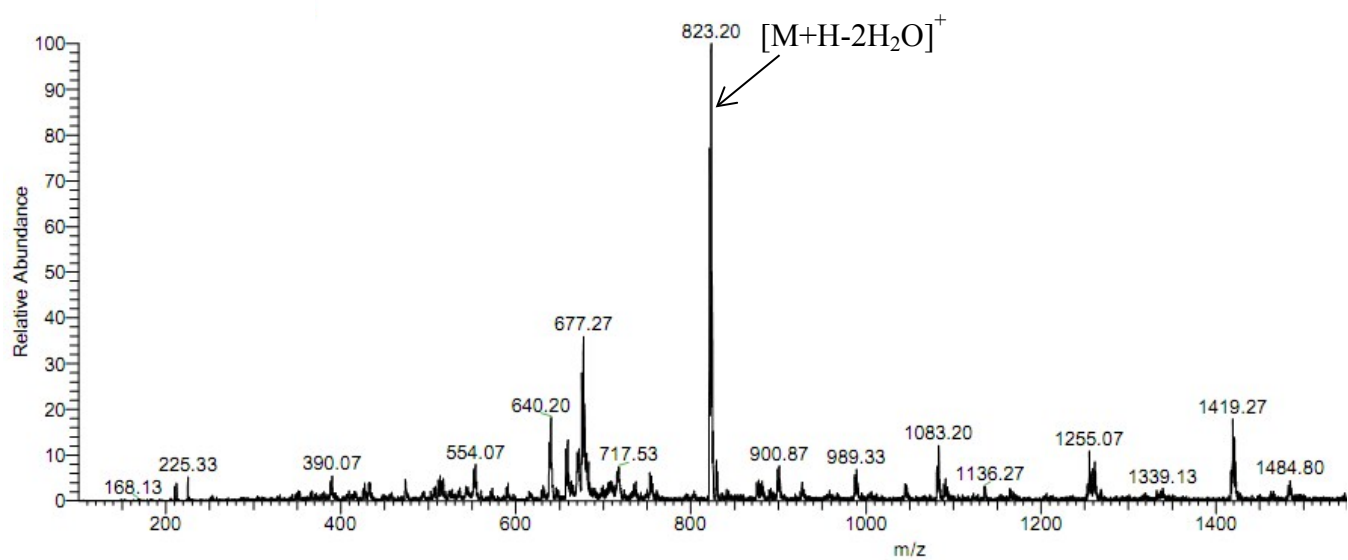


Figure S11. ESI-TOF mass spectrum of $[\text{Eu}(\text{DBM})_3(\text{H}_2\text{O})_2]$.

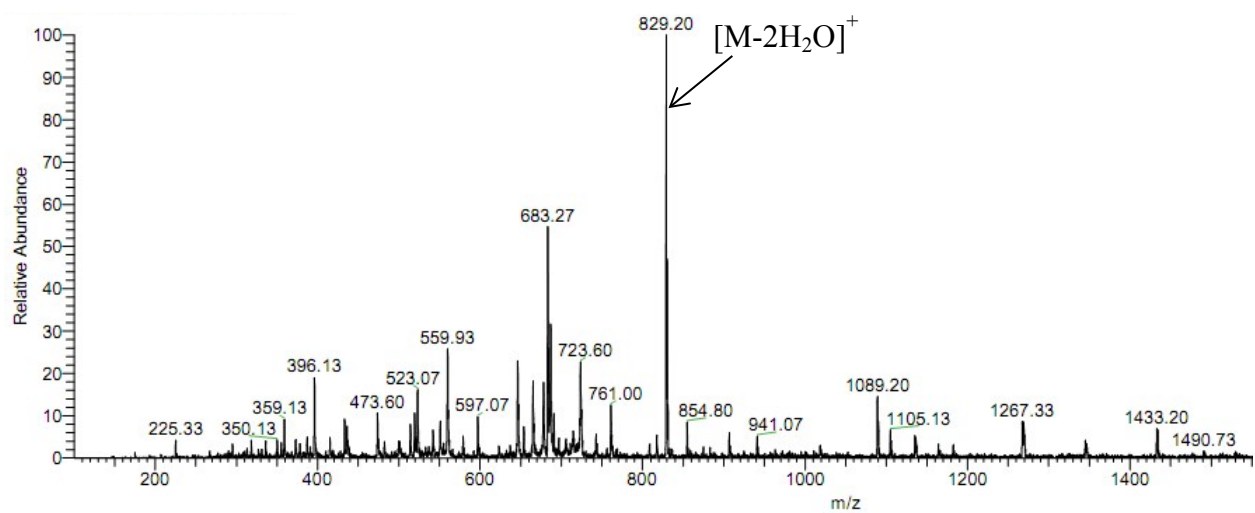


Figure S12. ESI-TOF mass spectrum of $[Tb(DBM)_3(H_2O)_2]$.

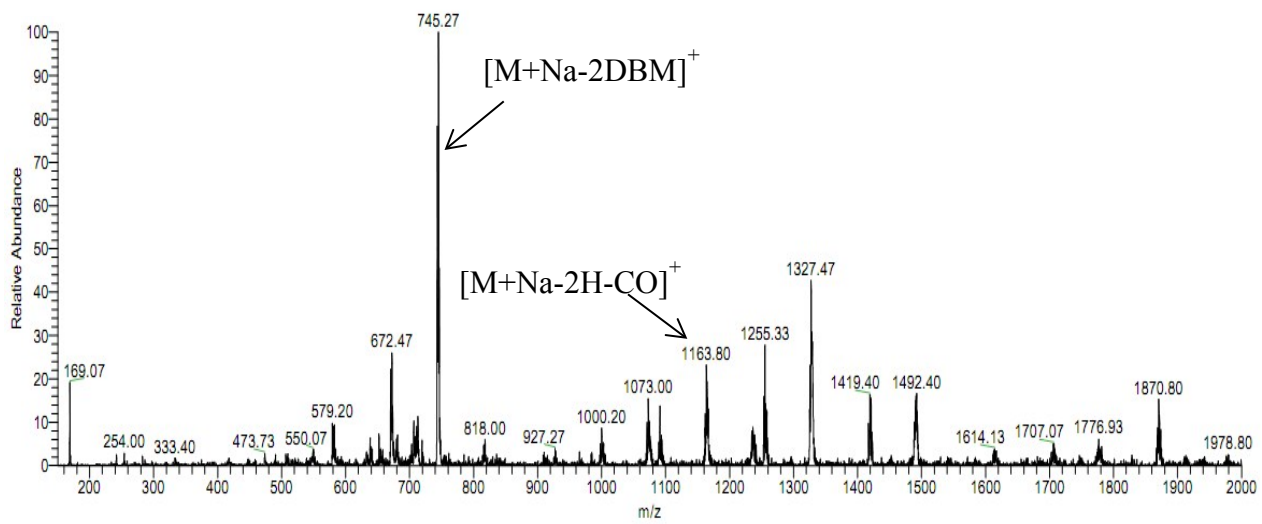


Figure S13. ESI-TOF mass spectrum of $[\text{Eu}(\text{DBM})_3(\text{L1})]$.

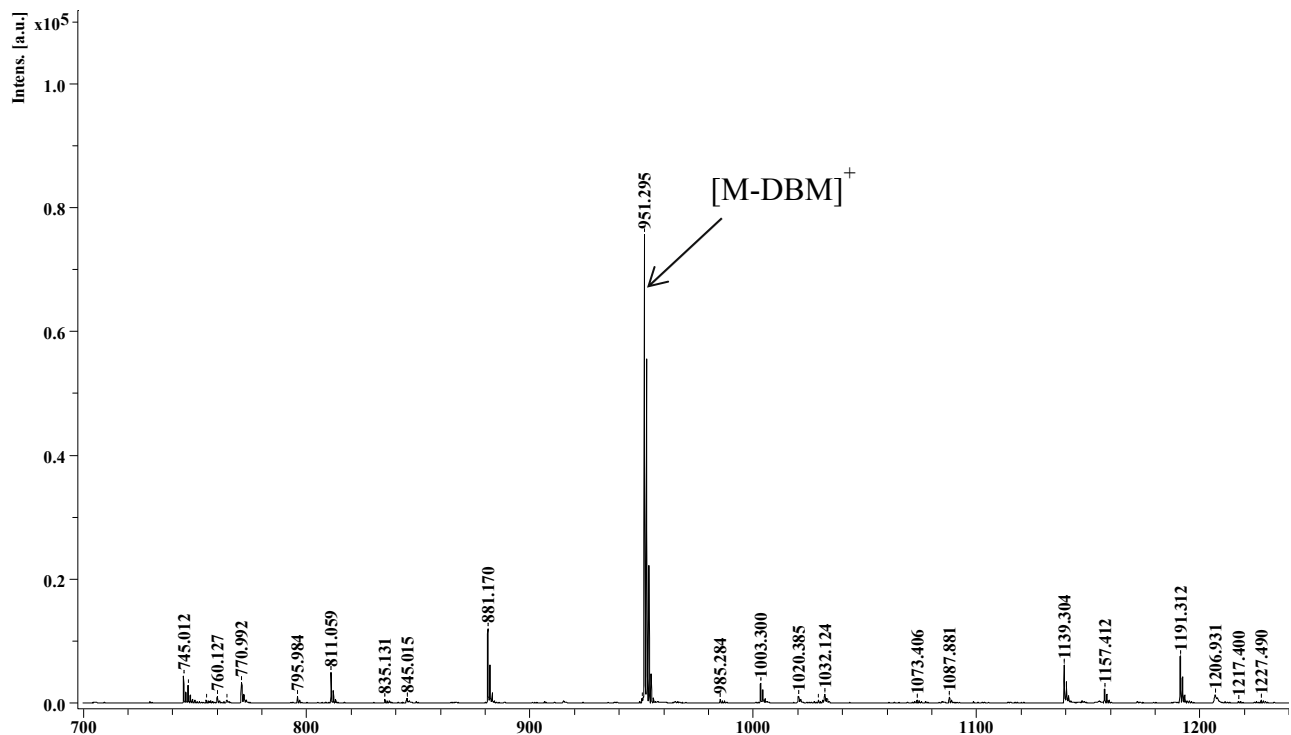


Figure S14. MALDI-TOF mass spectrum of $[\text{Tb}(\text{DBM})_3(\text{L1})]$.

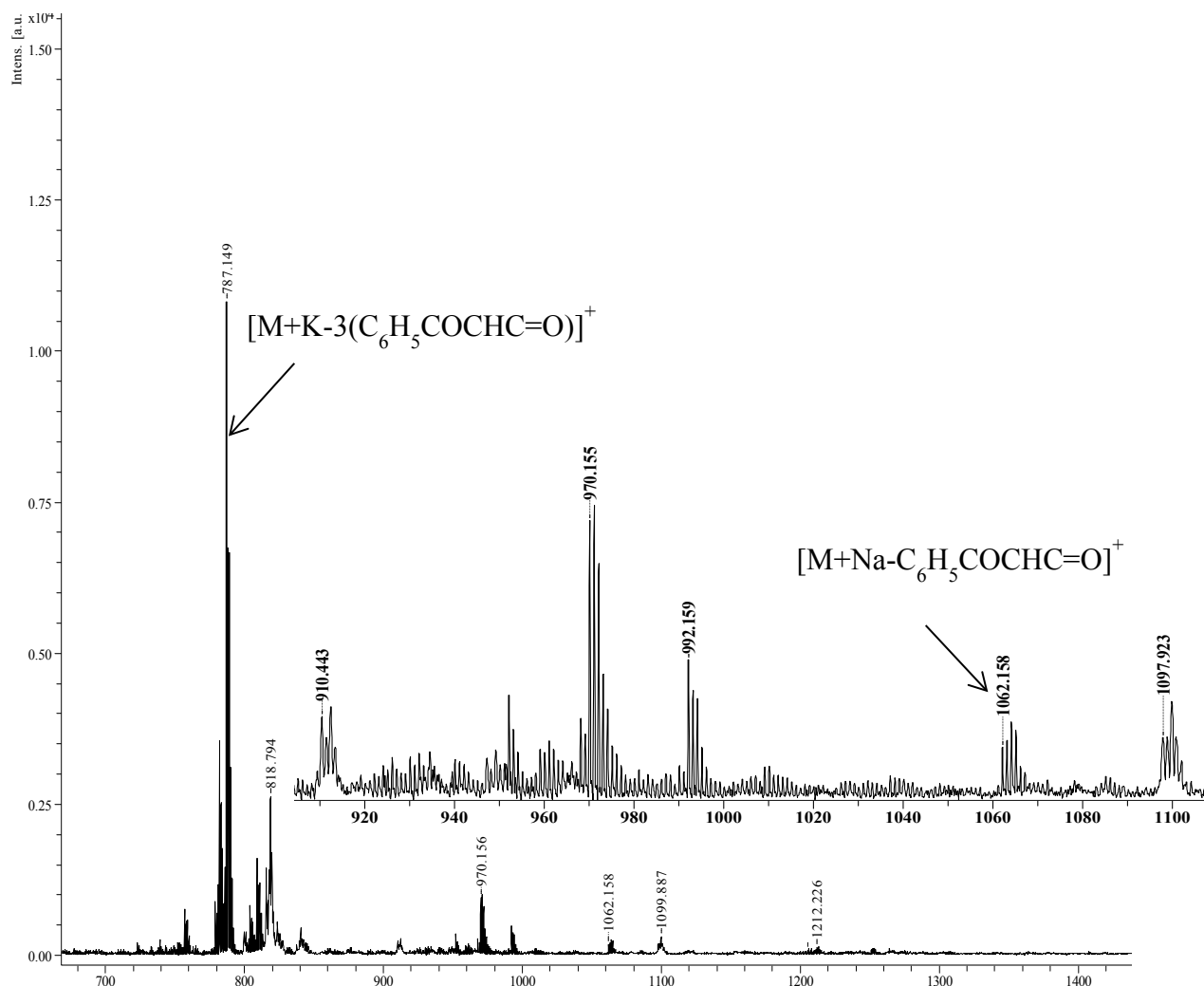


Figure S15. MALDI-TOF mass spectrum of $[\text{Eu}(\text{DBM})_3(\text{L2})]$.

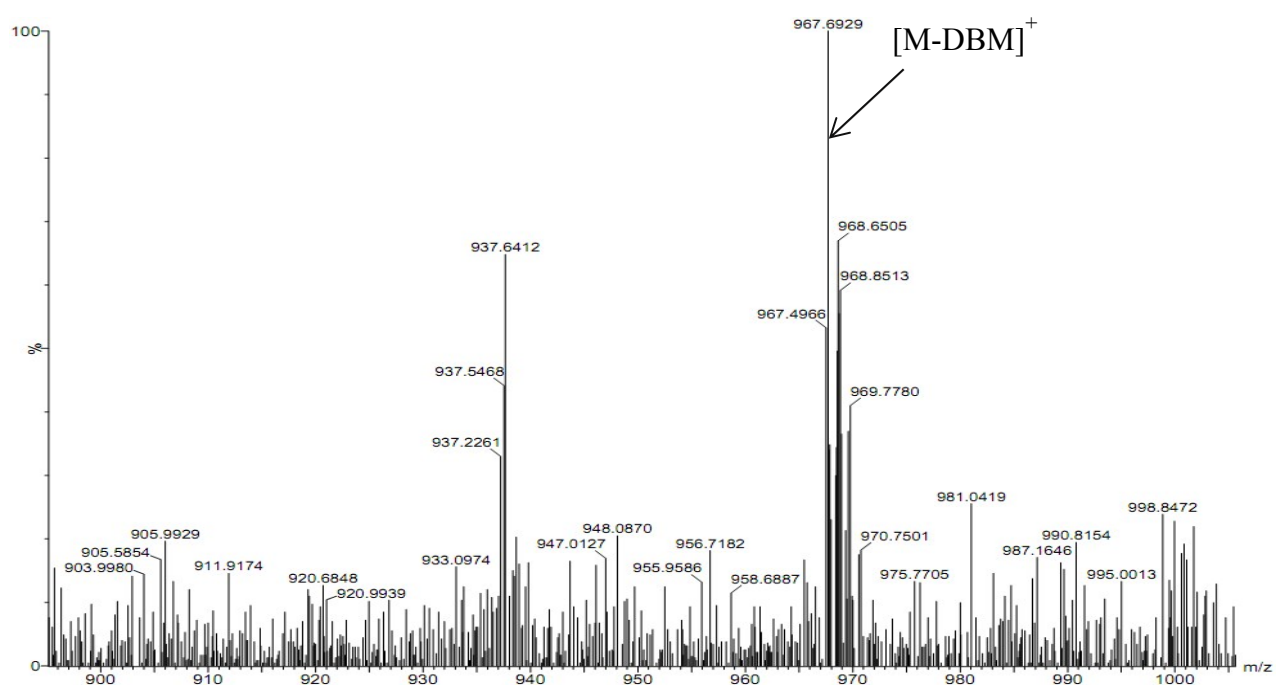


Figure S16. ESI mass spectrum of $[\text{Tb}(\text{DBM})_3(\text{L2})]$.

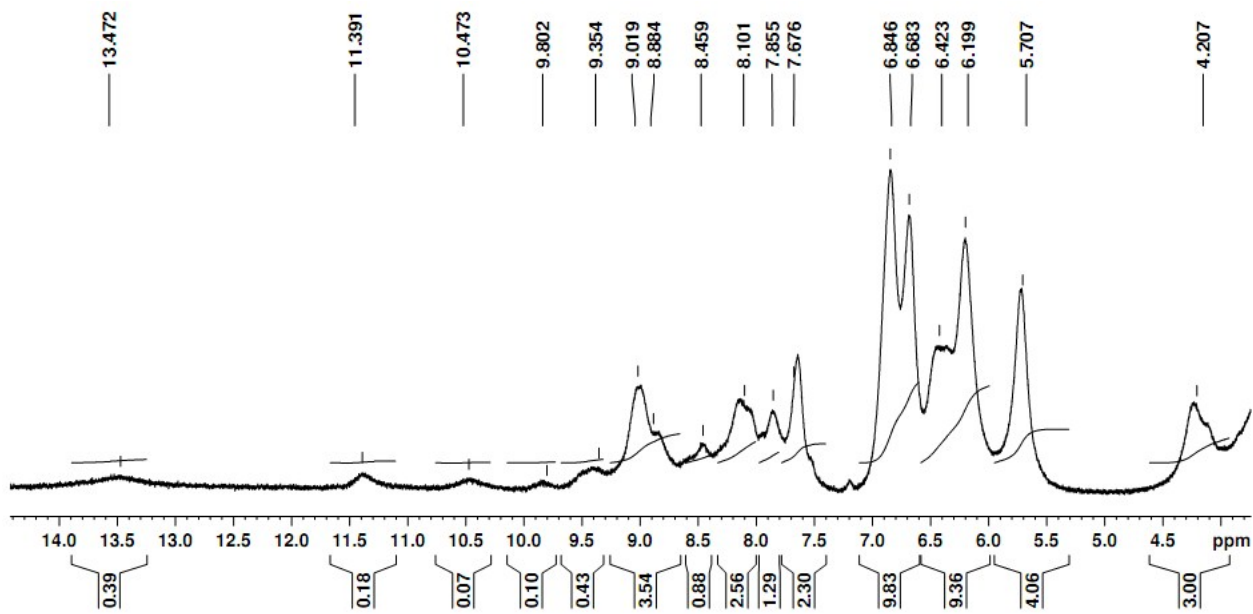


Figure S17. 500 MHz ^1H NMR spectrum of $[\text{Eu}(\text{DBM})_3(\text{L1})]$ in $\text{DMSO}-d_6$ at 25 °C.

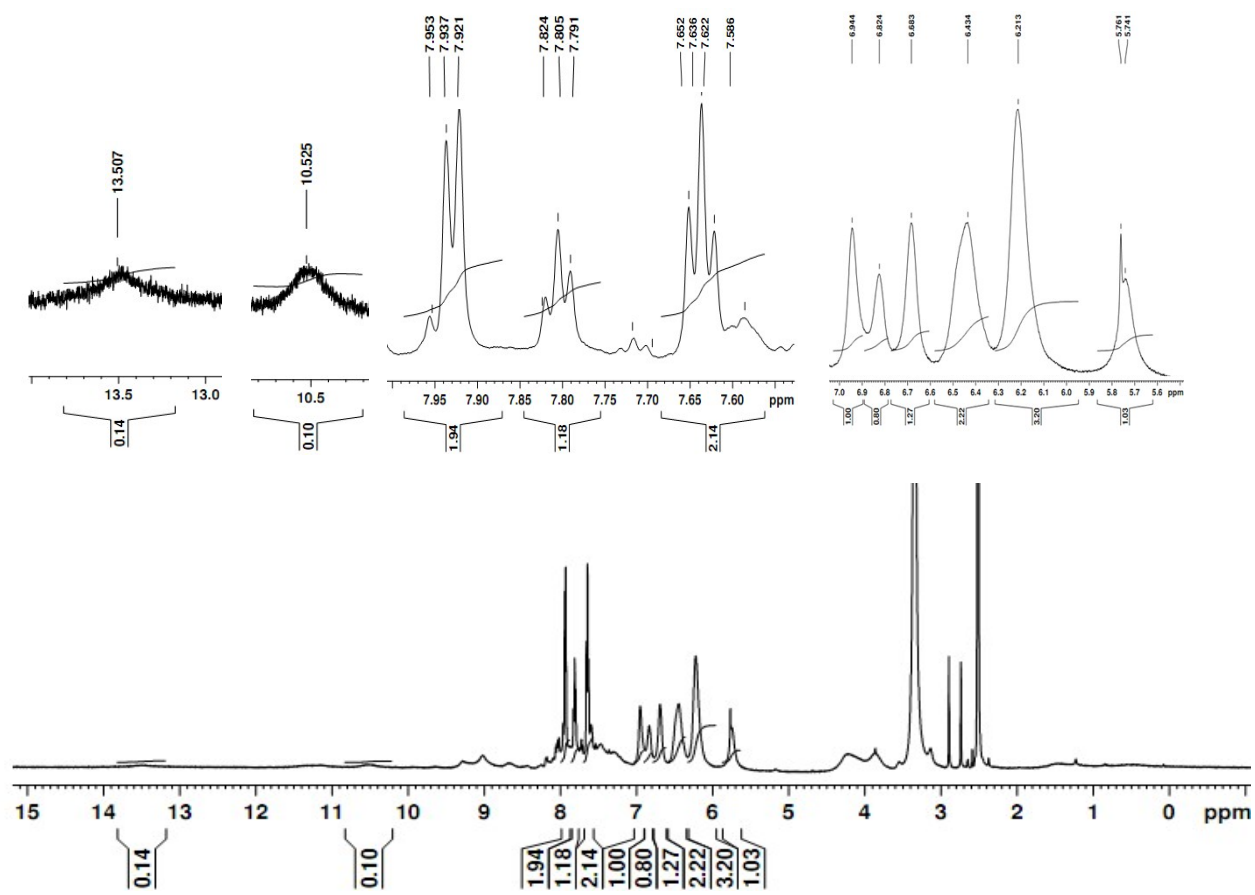


Figure S18. 500 MHz ^1H NMR spectrum of $[\text{Eu}(\text{DBM})_3(\text{L2})]$ in $\text{DMSO}-d_6$ at 25 °C.

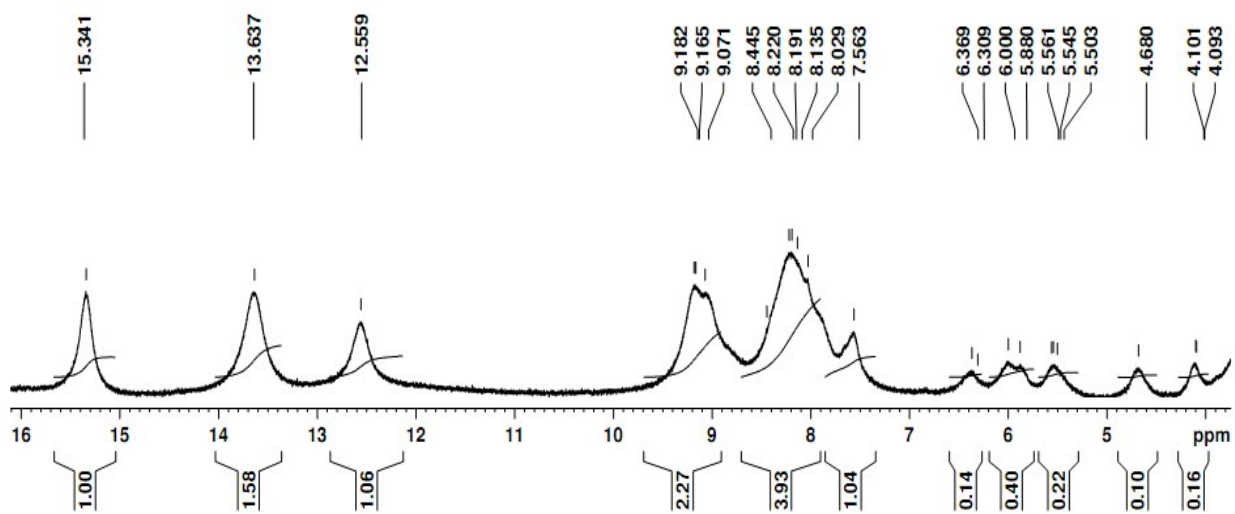


Figure S19. 500 MHz ^1H NMR spectrum of $[\text{Tb}(\text{DBM})_3(\text{L1})]$ in $\text{DMSO}-d_6$ at 25 °C.

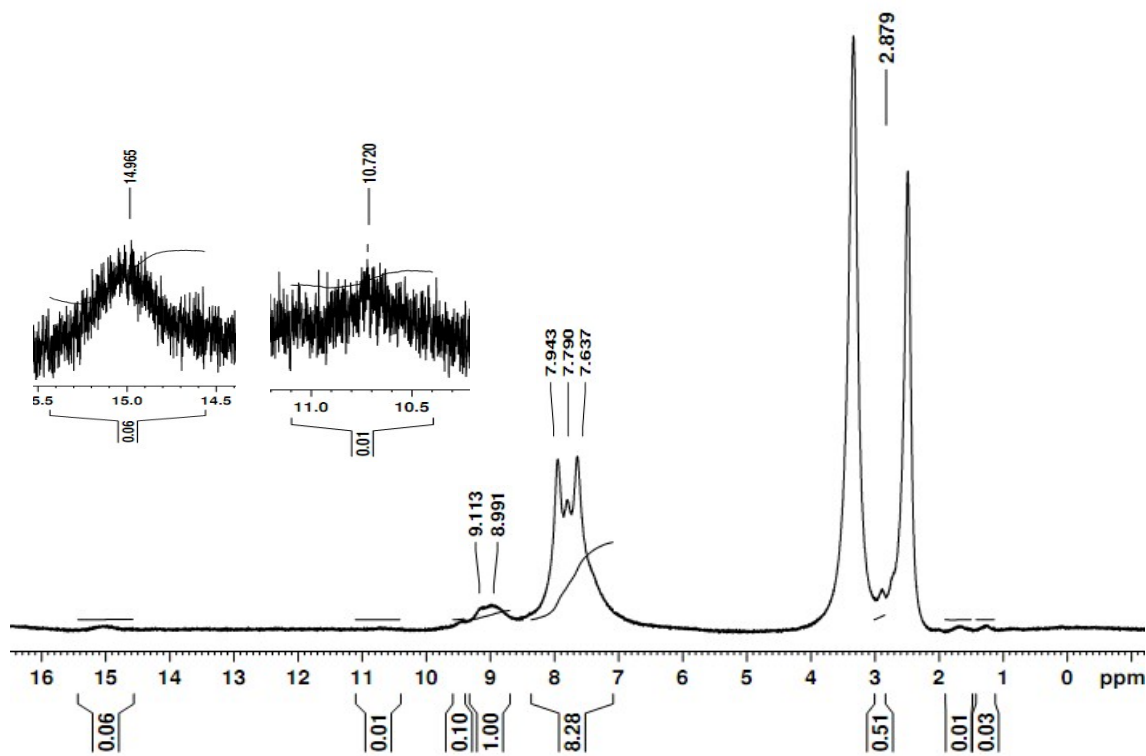


Figure S20. 500 MHz ^1H NMR spectrum of $[\text{Tb}(\text{DBM})_3(\text{L2})]$ in $\text{DMSO}-d_6$ at 25 °C.

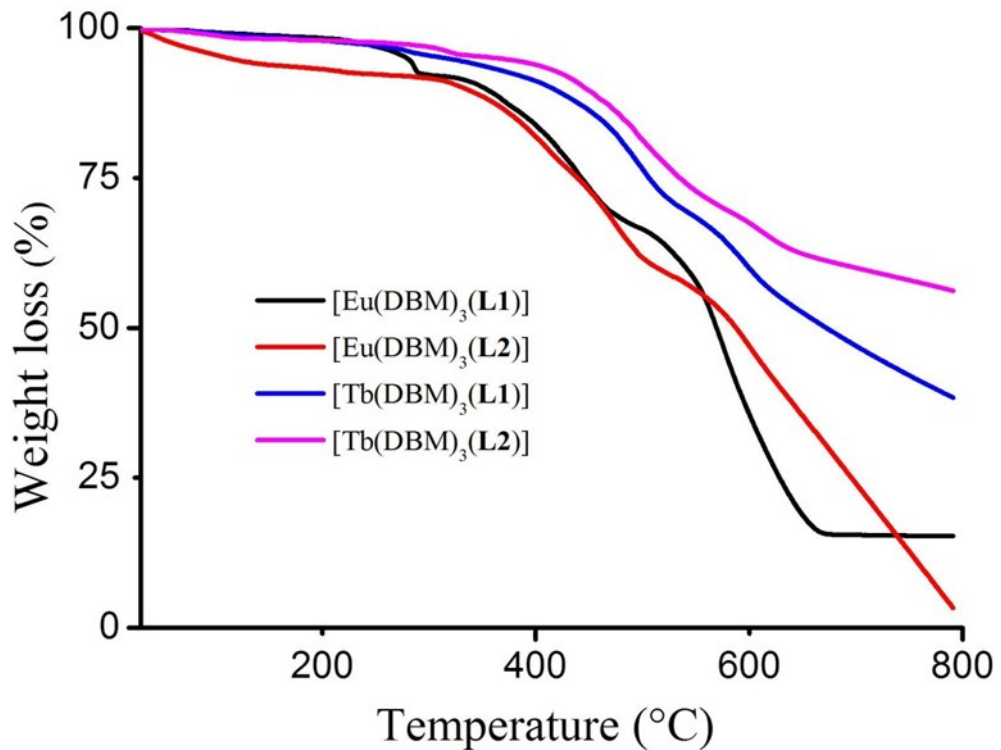


Figure S21. TGA curves of the complexes in N₂ atmosphere.

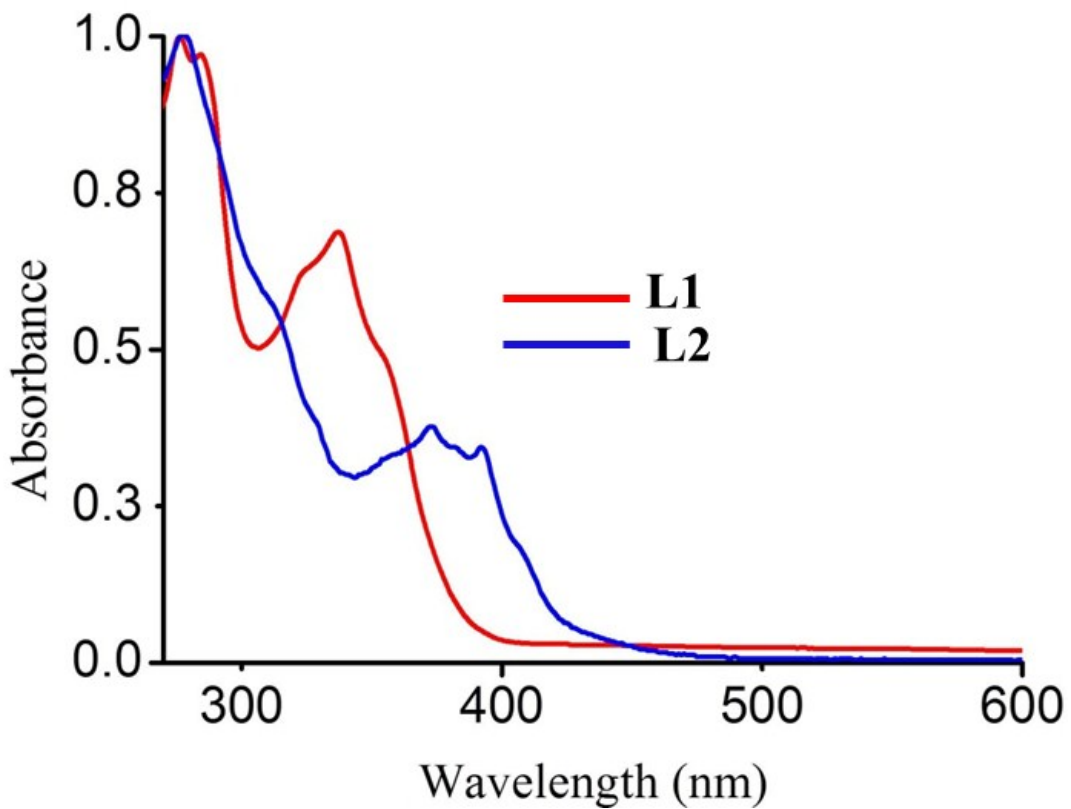


Figure S22. Electronic absorption spectra of **L1** and **L2**.

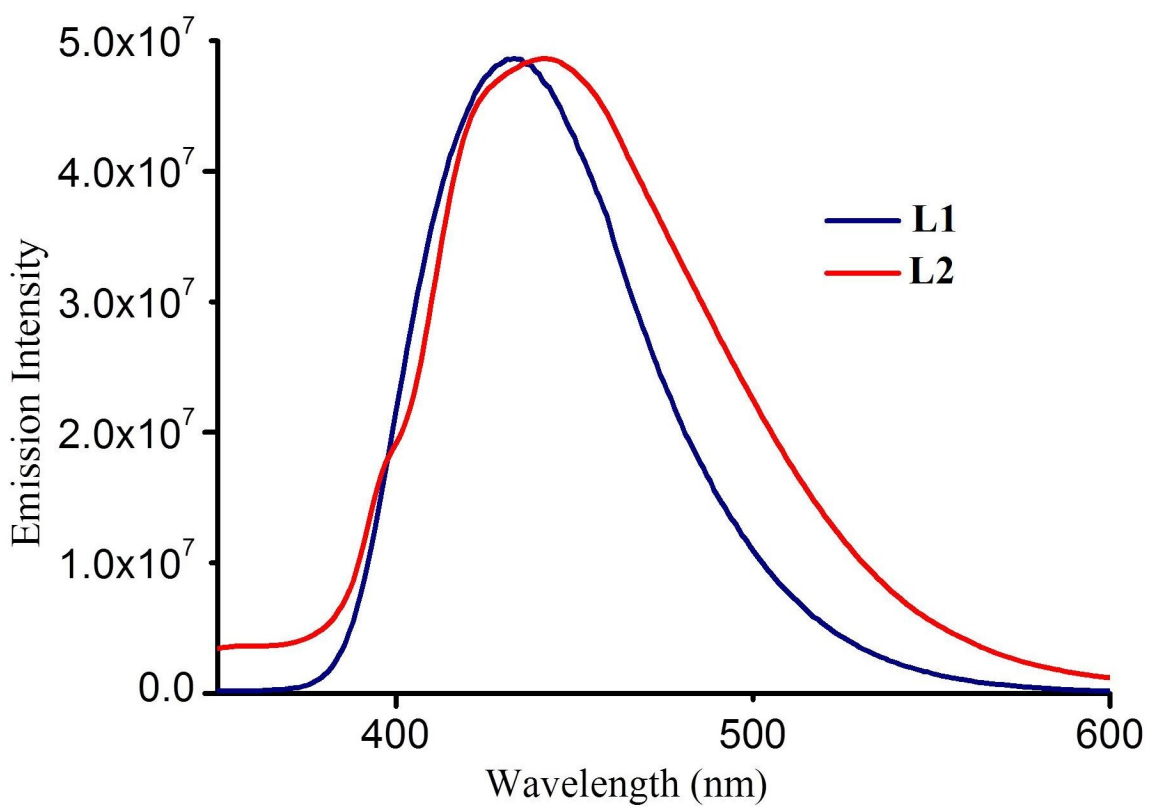


Figure S23. Photoluminescence spectra of **L1** and **L2** ($\lambda_{\text{ex}} = 278$ nm).

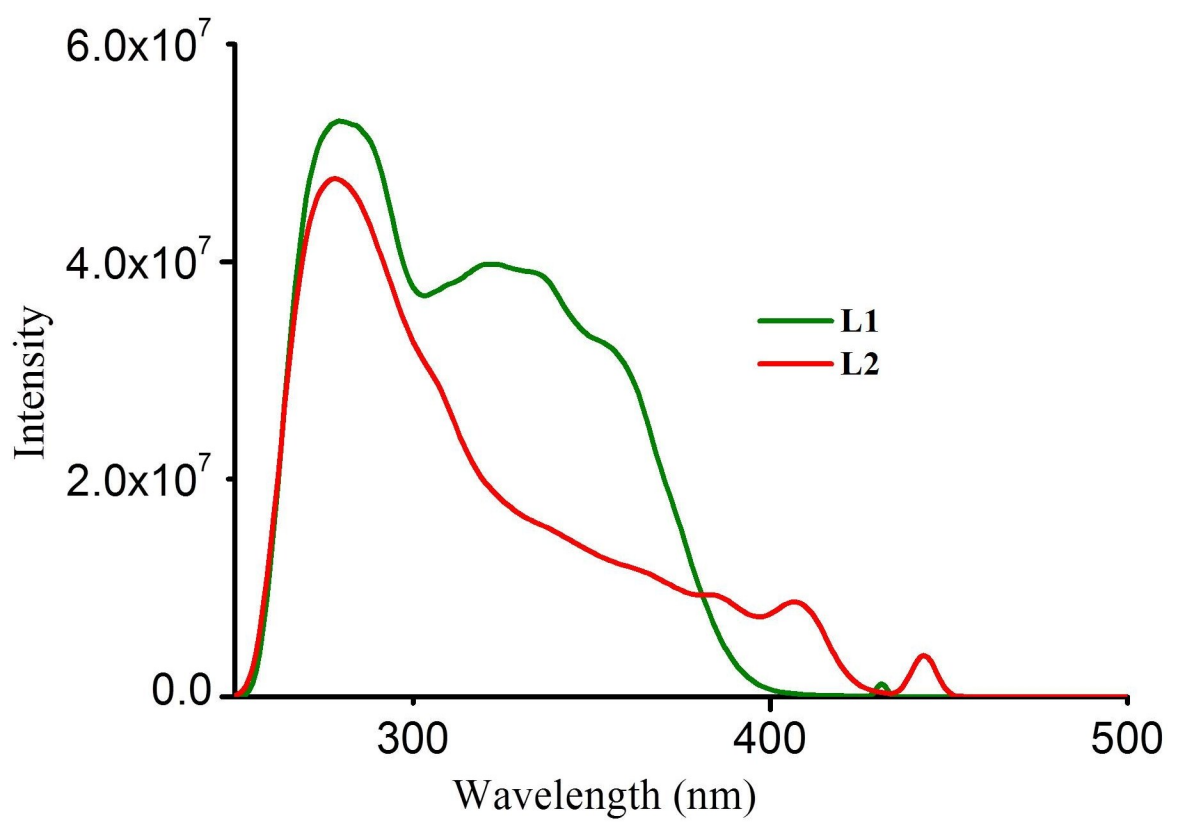


Figure S24. Excitation spectra of **L1** and **L2**.

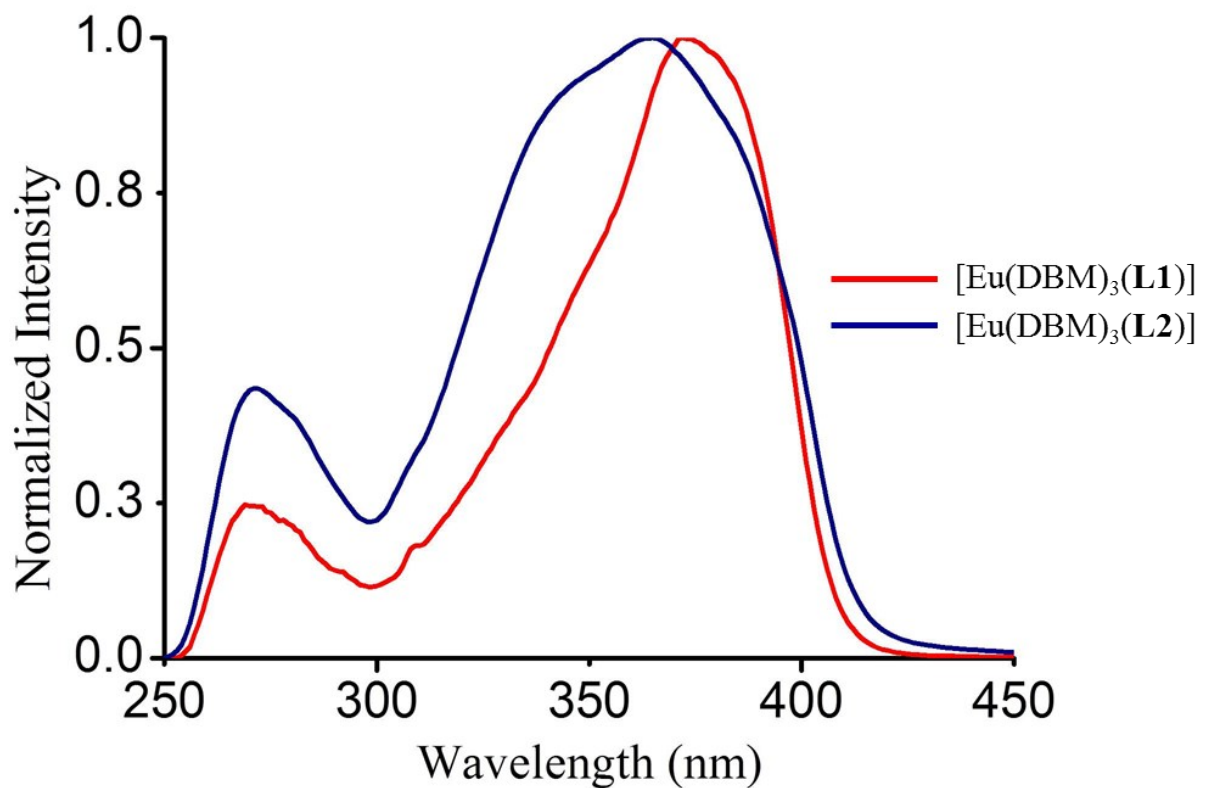


Figure S25. Excitation spectra of $[\text{Eu}(\text{DBM})_3(\text{L1})]$ ($\lambda_{\text{ex}} = 372$ and 269 nm) and $[\text{Eu}(\text{DBM})_3(\text{L2})]$ ($\lambda_{\text{ex}} = 365$ and 271 nm).

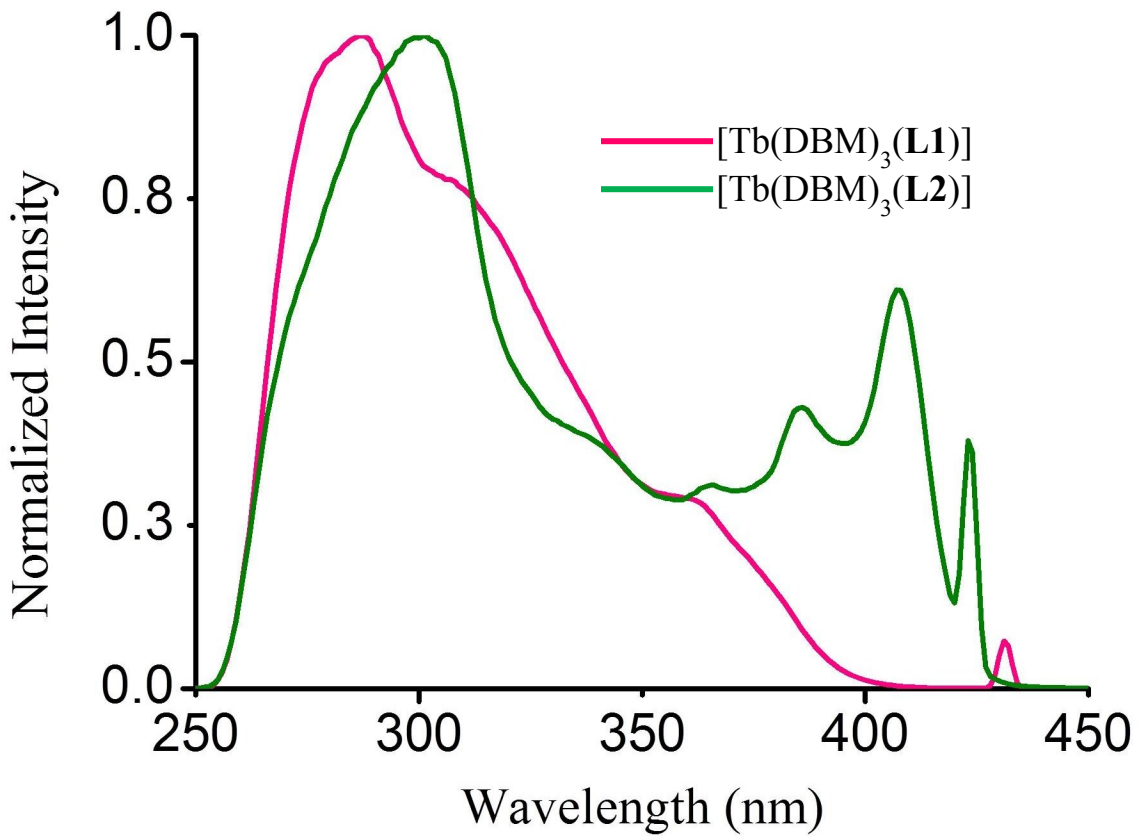


Figure S26. Excitation spectra of $[\text{Tb}(\text{DBM})_3(\text{L1})]$ ($\lambda_{\text{ex}} = 362, 307$, and 287 nm) and $[\text{Tb}(\text{DBM})_3(\text{L2})]$ ($\lambda_{\text{ex}} = 407, 386, 365$ and 2301 nm).

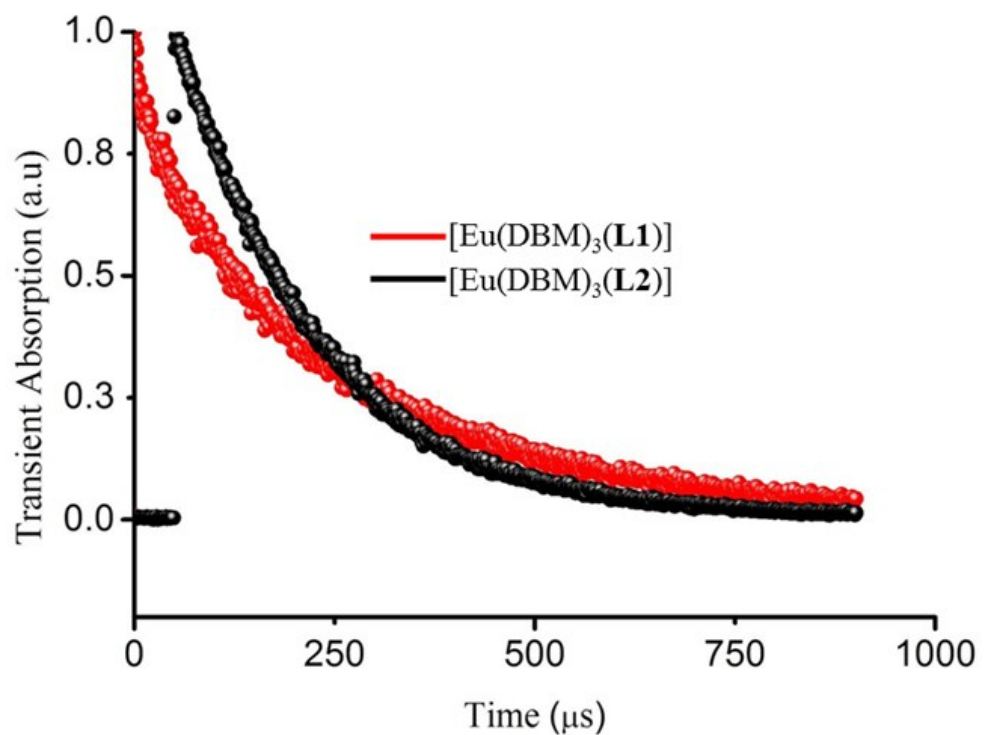


Figure S27. Luminescence decay curves of $[\text{Eu}(\text{DBM})_3(\text{L1})]$ and $[\text{Eu}(\text{DBM})_3(\text{L2})]$ in C_6D_6 .